



ELSEVIER

Available online at www.sciencedirect.comJournal of volcanology
and geothermal research

Journal of Volcanology and Geothermal Research xx (2006) xxx–xxx

www.elsevier.com/locate/jvolgeores

Hydrothermal circulation at Mount St. Helens determined by self-potential measurements

Paul A. Bedrosian^{a,*}, Martyn J. Unsworth^{b,1}, Malcolm J.S. Johnston^{c,2}

^a U.S. Geological Survey, Denver Federal Center, MS 964, Denver, Colorado, 80225, United States

^b Department of Physics, University of Alberta, Edmonton, Alberta, Canada T6G 2J1

^c U.S. Geological Survey, 345 Middlefield Rd., MS 977, Menlo Park, California, 94025, United States

Received 22 September 2005; received in revised form 17 August 2006; accepted 1 September 2006

Abstract

The distribution of hydrothermal circulation within active volcanoes is of importance in identifying regions of hydrothermal alteration which may in turn control explosivity, slope stability and sector collapse. Self-potential measurements, indicative of fluid circulation, were made within the crater of Mount St. Helens in 2000 and 2001. A strong dipolar anomaly in the self-potential field was detected on the north face of the 1980–86 lava dome. This anomaly reaches a value of negative one volt on the lower flanks of the dome and reverses sign toward the dome summit. The anomaly pattern is believed to result from a combination of thermoelectric, electrokinetic, and fluid disruption effects within and surrounding the dome. Heat supplied from a cooling dacite magma very likely drives a shallow hydrothermal convection cell within the dome. The temporal stability of the SP field, low surface recharge rate, and magmatic component to fumarole condensates and thermal waters suggest the hydrothermal system is maintained by water vapor exsolved from the magma and modulated on short time scales by surface recharge.

© 2006 Elsevier B.V. All rights reserved.

Keywords: self-potential; fluid flow; Mount St. Helens; hydrothermal circulation

1. Introduction

Mount St. Helens is a young stratovolcano whose recent eruptive history includes the lateral blast and Plinian eruption of May, 1980 (Lipman and Mullineaux, 1981). Subsequent eruptions from 1980–86 built a kilometer-wide dacite dome which cooled for nearly two

decades (Swanson et al., 1987; Swanson and Holcomb, 1990) until dome-building resumed in the fall of 2004, approximately 500 m south of the 1980–86 dome. The newly extruded dome of the current eruptive sequence reached a volume half that of the 1980–86 dome as of February, 2005 (Major et al., 2005). Since 1983 there has been continuous fumarolic activity on the 1980–86 dome, though it is unclear whether such activity is related to a shallow hydrothermal cell within the dome or the boiling of a deep water table (Hurwitz et al., 2003). Furthermore, hot, mineral-rich waters emerge through a series of springs and seeps within the breach, the 1–2 km² region north of the dome exposed by the lateral collapse of May 18, 1980. While these surface observations give indications of hydrothermal activity within the crater of Mount

* Corresponding author. Tel.: +1 303 236 4834; fax: +1 303 236 1425.

E-mail addresses: pbedrosian@usgs.gov (P.A. Bedrosian), unsworth@Phys.UAlberta.CA (M.J. Unsworth), mal@usgs.gov (M.J.S. Johnston).

¹ Tel.: +1 780 492 3041; fax: +1 780 492 0714.

² Tel.: +1 650 329 4812; fax: +1 650 329 5163.

St. Helens, the existence, depth, distribution, and stability of such hydrothermal cells is unknown.

The self-potential (SP) method is a geophysical technique employed in many applications, including mineral and geothermal exploration, environmental investigations, and volcanic studies (Nyquist and Corry, 2002). In a SP survey, small voltages generated by geochemical reactions, fluid flow, or temperature variations are measured at the Earth's surface. Active volcanoes commonly exhibit regional SP anomalies greater than 1 V (for example, Mt. Unzen in Japan (Hashimoto and Tanaka, 1995); La Fournaise on Reunion Island (Michel and Zlotnicki, 1998). Stronger 2–3 V anomalies have been measured on Mt. Fuji in Japan (Aizawa et al., 2005) and Agadak volcano in Alaska (Corwin and Hoover, 1979), and a 4 V anomaly was reported on Misti Volcano in Chile (Thouret et al., 2001; Finizola et al., 2004). Self-potential measurements are primarily used to map lithologic boundaries (e.g., faults, dikes, buried caldera structures) and infer circulation patterns of subsurface fluids (Zlotnicki et al., 1998; Aubert et al., 2000; Revil et al., 2004). In addition to spatial variations, temporal variations have been observed prior to eruptions (Miyake-jima, Sasai et al. (2002); Mount Etna, Lénat (1995)), coincident with volcanoseismic tremors (Byrdina et al., 2003), and during fumarole activity (Aizawa, 2004). The self-potential method is finding increased use as an important volcano monitoring technique.

The self-potential anomalies measured on volcanoes are believed to be due to a combination of electrokinetic, thermoelectric, and fluid disruption effects. In the electrokinetic (EK) effect, an electric field is generated as fluids move through a porous medium (Nourbehecht, 1963) and is believed to be a major contribution to the strong SP anomalies measured on active volcanoes. Chemical complexation at the mineral/pore water interface gives rise to a charge separation, and hence a net current density, during flow of the pore fluid (Revil et al., 1999). This is the opposite of electro-osmotic flow, in which an applied electric field generates fluid flow via viscous coupling of free charges and the pore fluid (Pretorius et al., 1974). For both phenomena, the sign of the generated voltage, in relation to fluid flow direction, is determined by the zeta potential, a proportionality constant which takes into account the electrochemical properties of the matrix/pore water interface. For most earth materials, the zeta potential is negative, resulting in positive voltages for upward fluid flow. In volcanic systems, EK voltages are thought to result from convective hydrothermal cells that are sustained by magma at shallow depths. The electrokinetic effect also generates self-potentials in the absence of

geothermal activity due to the topographically-driven flow of groundwater. The resulting SP signal is correlated with topography, allowing it to be distinguished from signals of geothermal origin (Jackson and Kauahikaua, 1987). Thermoelectric (TE) effects can also produce voltage gradients arising from the Soret effect, in which differential diffusion of ions in a pore fluid is imposed by a thermal gradient. Though probably a contributing factor, the thermoelectric effect, known to produce SP anomalies of up to ~200 mV (Corwin and Hoover, 1979), does not explain the much larger anomalies measured on volcanoes throughout the world. Rapid fluid disruption (RFD), suggested by Johnston et al. (2001, 2002), is a two-phase charge separation mechanism capable of producing significant self-potentials during vaporization as hot rock comes into contact with subsurface fluids. Depending on the degree of vaporization, either positive or negative potentials may be generated, and may explain the presence of SP anomalies in hot, dry regions where fluid flow is unexpected. While there is disagreement over the role and necessity of RFD in explaining volcanic SP anomalies (Revil, 2002), Johnston et al. (2002) have shown in no-flow experiments that RFD is capable of producing large potentials (up to several volts).

Several previous SP studies have been undertaken at Mount St. Helens. Continuous recording of the self-potential on the volcano's east flank was made over a two year period beginning in September, 1980, four months after the paroxysmal May eruption (Davis et al., 1989). Significant SP changes were measured during the last major pyroclastic eruption (October 16–18, 1980), however, these measurements used only a few electrodes, and it is not known if the potential changes were due to volcanic processes or simply rainwater flowing over the electrodes. This is an inherent limitation of monitoring temporal variations of the self-potential field with a limited number of electrodes. Separating local electrode noise from volcanic signals requires repeated SP surveying with significant spatial coverage. Measurements of this kind were initiated at Mount St. Helens in 1982. A SP survey extended from the south crater wall to a location 2 km north of the then forming dome, with 100 m spacing between measurement locations (Dan Dzurisin, pers. comm.). These measurements revealed a positive anomaly near the dome and along the axis of the breach. An east–west trending negative anomaly was also noted along the rampart, a pronounced step in topography ~1 km north of the dome.

This paper describes self-potential surveys within the crater during 2000–2001, prior to the recent and continuing dome-building event that began in 2004. A

strong dipolar anomaly was measured on the north face of the 1980–86 dome. The origin of this anomaly is discussed in terms of electrokinetic, thermoelectric, and fluid disruption effects, and implications for the shallow plumbing of the volcano are discussed.

2. Self-potential measurements

The self-potential survey began in August 2000, 14 years after the last dome-building event. The primary goals of these measurements were to map the self-potential field of the crater as a baseline for future monitoring efforts and to determine the extent of hydrothermal circulation in the vicinity of the 1980–86 dome. SP data were collected over a one-week period in August 2000 along a series of profiles (Fig. 1, BB', CC', DD') on the breach and northern flank of the dome. Data coverage on and around the dome was limited by rockfall hazards from the dome and crater walls. SP data were additionally acquired along profile AA', continuing north from location B, resulting in a combined 2.5 km

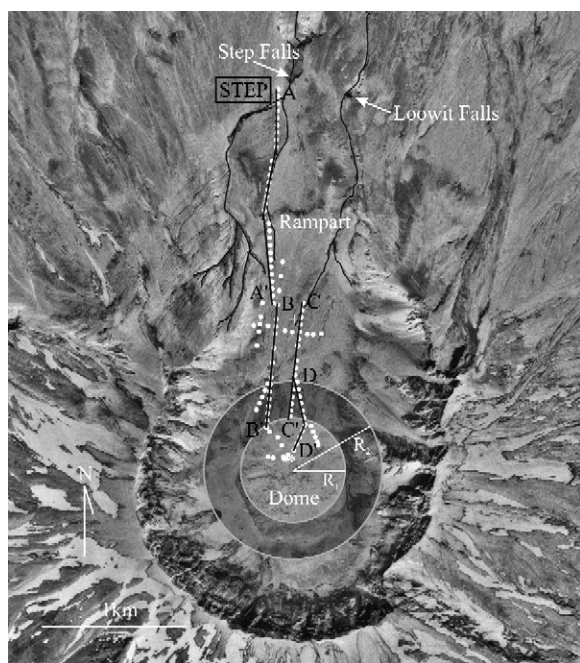


Fig. 1. Crater of Mount St. Helens in summer 1994 showing the breached northern flank and 1980–86 composite lava dome. White circles denote 2000 SP measurement locations grouped along profiles AA', BB', CC', and DD'. Additional measurements made in 2001 include the eastern spur off profile DD' and a series of spot measurements near the dome summit. Radii R_1 and R_2 are measured from the dome summit and are discussed in the text. Asterisk (*) denotes the location of fumaroles at the time of the survey; plus (+) symbols indicate locations where thermal waters were sampled. Major geomorphic features are noted.

profile from the top of Step Falls to within 100 m of the dome summit. Measurements were made using a high input-impedance (10 M Ω) voltmeter and a pair of Pb/PbCl₂ porous-cap electrodes. A second survey in September 2001 collected additional data in the vicinity of the dome after repeating measurements along profile DD' to determine if time-variations in the SP field were significant. In both surveys, self-potential measurements were made every 50 m using an expanding dipole setup with a fixed base station (Corwin and Hoover, 1979). The running electrode was loosely planted during the measurements in one of 2–4 shallow holes spread throughout a 1 m² area. Measurements made in this manner allow the variability in the self-potential at each location to be assessed and permit computation of a standard error.

The main sources of error in self-potential exploration are (a) contamination from telluric signals and (b) electrode polarization. To determine the effect of telluric signals on the measured data, a fixed-length dipole was deployed parallel to the SP dipole. Several days of monitoring the fixed dipole showed the telluric effects to be negligible over the time scale of our measurements. To account for electrode polarization, the two electrodes were placed in a saturated salt water bath and the potential between them measured at the beginning and end of a series of measurements. A linear drift correction was then applied to all intermediate measurements. In 2001, direct comparison with a pair of high stability (polarization <1 mV) electrodes verified that electrode polarization was a minor contribution and was adequately removed through the applied drift correction. Standard errors in the measurements are dominantly the result of the highly variable lithology within the breach, due in turn to the juxtaposition of numerous debris flows, surge deposits, and rockfalls.

Covering the northwest flank of the dome required taking measurements on snow. A small quantity of salt (<200 g) and water were used to reduce the contact resistance to a reasonable value (~500 k Ω two-way averaged resistance). The measurements on snow proved repeatable, varied smoothly from site to site, and generally had smaller standard deviations than measurements made on ash. As the dome is surrounded by snowfields on two sides, the ability to make SP measurements on snow is of importance to future surveys aimed at extending coverage of the dome.

Field measurements were taken relative to stations Step, B, and C, and all data were subsequently referenced to the northernmost station Step (Fig. 1). This station was chosen as a reference as it is furthest from suspected anomalies near the dome. Three levels of

averaging were employed to arrive at a final SP value for each location. Multiple measurements within each hole were first averaged. A weighted average was then used to average over the 2–4 holes at any given location. Finally, as most sites were reoccupied several times throughout the survey, a weighted average was taken over these measurements. Error propagation was applied to determine the standard deviation of the final reading; the average site deviation was 11 mV, though some locations have deviations as high as 50 mV. These errors represent less than 5%, and typically 1%, of the self-potential range (1500 mV) measured throughout the survey area.

3. SP observations

The general trend in the data is seen by examining the self-potential along four main profiles (labeled in Fig. 1) as a function of distance south of reference station Step (Fig. 2a). A prominent dipolar anomaly was measured on the north flank of the dome. This anomaly is visible on the three profiles covering the dome, with a magnitude three times that of all other variations within the survey area. A strong negative gradient (-9 mV/m) is observed on profiles BB', CC' and DD' before reversing sign on the upper flanks of the dome. Additionally, a

series of point measurements near the top of the dome continue the trend observed along the profiles.

The measured anomaly appears coincident with the break in topographic slope of the dome. Given the dome's symmetry, it is instructive to further examine the SP data as a function of radial distance from the dome summit, as shown in Fig. 2b. If our SP data are sampling part of a symmetric, dome-scale anomaly, we expect major changes in SP to occur at fixed radii along the three profiles covering the dome. Indeed, a SP minimum occurs at $R_1 = 360\text{--}430$ m along all profiles, and returns to a background value at $R_2 = 615\text{--}670$ m from the dome summit. Though consistent with a circular, dome-scale anomaly, the data alone do not require it.

It is possible the measured anomaly is limited to the north side of the dome, and simply reflects its composite nature. The 1980–86 lava dome is comprised of a series of overlapping extruded lobes, the boundaries of which may act as fluid pathways. Alternatively, between 1989 and 1991, a series of explosions issued from a vent on the north side of the dome (Mastin, 1994). This vent was believed to be located along an extensional fault that has subsequently been covered by lava and rockfall debris. It is thus possible the anomaly is associated with this buried vent. Additional SP data, however, collected in 2001 on the northeast flank of the dome (easternmost

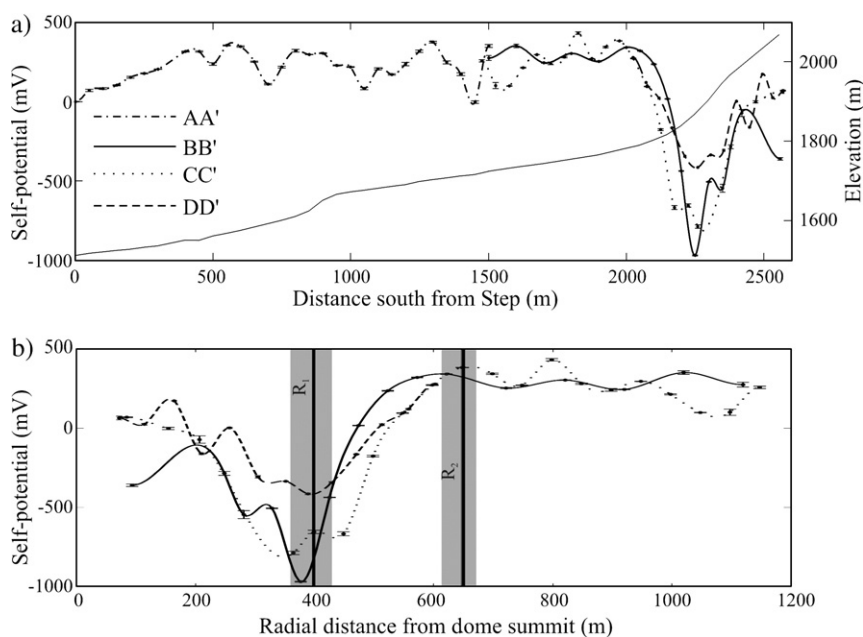


Fig. 2. Self-potential along sub-parallel profiles within the crater of Mount St. Helens. Potentials are referenced to the northernmost station Step. Error bars are shown at measurement locations. (a) Self-potential versus distance south of reference station Step. Thin solid line denotes elevation along profile AA'/BB'. (b) Self-potential for profiles covering the dome versus radial distance from the summit. Radii R_1 and R_2 characterize the peak magnitude of the negative anomaly and departure from the background field level, respectively. Light gray bars denote the range of these characteristic radii among the three profiles.

spur in Fig. 1) support the possibility of a dome-scale ring anomaly, showing a trend similar to the three profiles shown. Without additional measurements it is impossible to determine whether the measured anomaly is part of a larger dome-scale anomaly or is localized along the dome's north flank.

4. Interpretation and discussion

4.1. Topographic effect

Do our self-potential results indicate a topographic effect? This negative linear relationship between topography and self-potential is associated with groundwater flow, i.e., a gravity-driven hydrogeologic effect. It has been suggested that the resulting voltage varies with vadose zone thickness (Jackson and Kauahikaua, 1987). Modeling by Ishido (2004) concurs, finding that downward fluid flow in the vadose zone and underlying water table generates an observable topographic effect. Self-potential surveys on many volcanoes have measured potentials with gradients ranging from 1–10 mV per meter of elevation change (Hashimoto and Tanaka, 1995; Zlotnicki et al., 1998). Fig. 3 shows self-potential as a function of elevation for the four profiles shown in Fig. 2a. Despite the moderate topography, there is no consistent correlation between elevation and self-potential. Topographic effects are expected to be most

apparent far from the dome, where competing hydrothermal processes are not expected. Thus the breach region, with elevations ranging from 1500–1800 m, is most significant in assessing topographic effects. Rather than showing the negative slope expected from a topographic effect, the slope is slightly positive, as seen from the best-fit line to the data.

These data may indicate a vadose zone of relatively uniform thickness, possibly resulting from an impermeable boundary preventing flow from the vadose zone into a deeper water table (Finizola et al., 2002, 2004). Pyroclastic surge deposits, laid down during the 1980 eruption sequence, may form such a boundary. It is more probable, however, that the lack of a topographic effect within the crater of Mount St. Helens reflects a lack of meteoric influx. The strong topographic effects observed elsewhere have been on volcanoes with 4–12 m/yr of rainfall, far greater than the 1–2 m annual rainfall at Mount St. Helens, though comparable to further modeling by Ishido (2004) which produced a topographic effect. There may, however, be reason not to expect a topographic effect at Mount St. Helens. Based on the high permeability and low recharge rates of Cascade Range stratovolcanoes, Hurwitz et al. (2003) suggest the water table beneath these volcanoes may be quite deep. Furthermore, the authors argue that the presence of hydrothermal discharge high on the edifice implies that topographically-driven flow is restricted. Taken together,

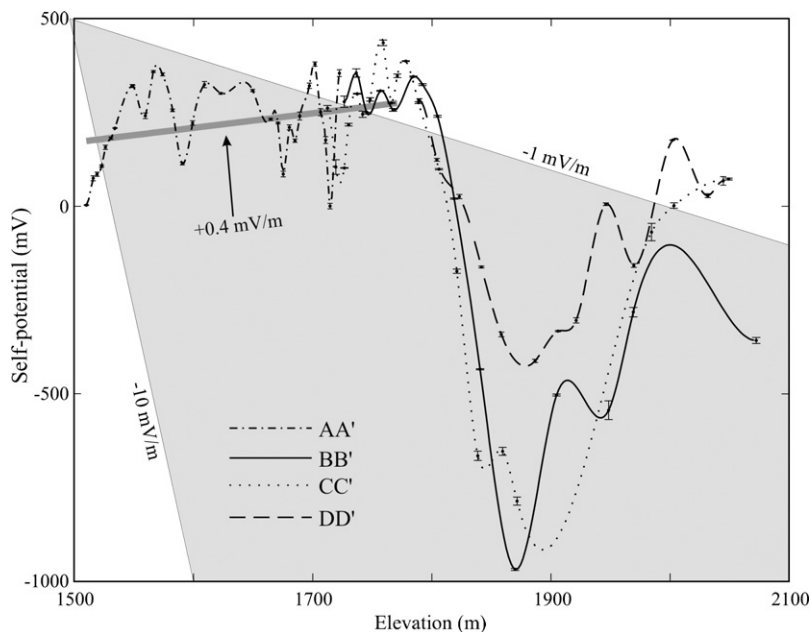


Fig. 3. Self-potential versus elevation for the four profiles shown in Fig. 2a. Potentials are relative to northernmost site Step, with adjacent points 50–100 m apart along the ground. Shaded area indicates the range of topographic gradients observed on other volcanoes, while thick gray line is the best-fit to SP data between 1500 m and 1800 m elevation, where competing mechanisms are unlikely.

the low rate of recharge, high permeability of the dome (Mastin, 1994), and high-elevation discharge through Loowit and Step Creeks offer a consistent explanation for the lack of an observed topographic effect within the crater of Mount St. Helens.

4.2. Source mechanisms

In discussing the cause of the measured anomaly, it is instructive to consider the depth of the likely source. As occurs with other potential field methods, the width of an observed self-potential anomaly is on the same order of magnitude as the depth to its source. As discussed previously, the measured anomaly may represent part of a negative ring anomaly centered about the dome with a diameter of ~ 1300 m, encircling a positive disc of ~ 800 m diameter (Figs. 1 and 2b). The source is thus located at relatively shallow depth (<1.5 km). This represents a maximum source depth, as the measured anomaly is only mapped for ~ 600 m, suggesting an even shallower source beneath the north flank. Regardless, the causative mechanism is likely to be confined to within or just below the kilometer-wide dome.

What is known about the thermal structure of the composite dome? A strong heat source is suggested by the continuous fumarolic activity on the dome. During the 2001 survey, gas temperatures of 60° – 85° °C were measured at several fumaroles on the north flank. A shallow heat source was further inferred from repeated magnetic measurements by Dzurisin et al. (1990), who estimated the magnetized carapace was growing at a rate of 2–4 cm/day. Extrapolating the authors' findings to 2000 gives an expected Curie depth ($T > 300^{\circ}$ °C) of 75–150 m. Evidence for a shallow heat source also comes from the Loowit hot springs and a series of high temperature seeps leading into Step Creek.

The source of the dipole anomaly thus lies at relatively shallow depths within a hot dome. Possible generating mechanisms include thermoelectric effects and processes related to hydrothermal circulation, i.e., requiring water and/or water vapor. A thermoelectric contribution to the central positive anomaly is expected, as elevated temperatures occur at shallow depths within the dome. Thermoelectric coupling coefficients, however, are typically a few tenths of a mV/°C and rarely produce anomalies larger than 200 mV (Corwin and Hoover, 1979). Despite the high temperature of a near-surface dacite melt (930° °C, Rutherford et al., 1985), it is unlikely that the thermoelectric effect alone produces the abrupt upturn from nearly -1000 mV on the lower flanks to $+300$ mV on the upper flanks of the dome. Further-

more, thermoelectric effects cannot adequately explain the large negative potentials measured.

Rapid fluid disruption effects can likewise generate positive potentials during vaporization (Johnston et al., 2001, 2002), and the necessary elevated temperatures are present beneath the dome of Mount St. Helens. Rainfall percolating down to hot dacite will be vaporized, as well as waters exsolved from a slowly crystallizing subsurface melt. Given the persistence of fumaroles on the dome and the progressive magnetization of the dome, it is hard to argue that RFD does not contribute to some degree. Revil (2002) have argued that potentials attributed to the RFD mechanism can alternatively be described solely by electrokinetic effects. Measurements by Johnston et al. (2002), however, using samples of the Mount St. Helens dacite under conditions relevant to the 1980–86 dome, found that vaporization produced RFD potentials much larger than EK potentials generated during fluid flow. RFD may thus be the dominant mechanism giving rise to the positive potentials over the dome summit. Again, however, it is difficult to explain the large negative potentials with the RFD mechanism.

The negative self-potential observed on the lower flanks of the dome can only be explained via the electrokinetic effect, and hence implies subsurface fluid flow. We wish to emphasize that, though this region shows a clear correlation with topography, we do not consider it to be a topographic effect as it is localized and clearly associated with hydrothermal activity.

The direction of fluid flow is dependent on the sign of the zeta potential. While Hase et al. (2003) found samples from Aso caldera, Japan with positive zeta potentials, measurements on the Mount St. Helens dacite are more conventional, with a zeta potential averaging -29 mV/bar. Thus the negative self-potentials arise from downward fluid flow within or along the flanks of the dome. Furthermore, such fluid flow is limited to the outer ~ 100 m of the dome by the thermal constraints described in the magnetic study of Dzurisin et al. (1990). The EK effect probably contributes to the central positive anomaly as well, in a source region located between the surface and the vaporization isotherm.

4.3. Circulation model

The prominent dipolar anomaly reflects a combination of TE, RFD, and EK effects. More importantly, these results imply movement of fluids and vapor within the 1980–86 lava dome. Possible sources for these fluids include meteoric recharge, magmatic waters released from a cooling dacite melt, and groundwater from a

presumably deep water table. Sampling of dome fumarole condensates suggests a simple mixing between exsolved magmatic water vapor and local meteoric waters, with between 30 and 70% magmatic input (Shevenell and Goff, 1993). A magmatic component is also present in the thermal waters of Loowit creek, though 90% of its waters are meteoric in origin. The mixing of groundwater cannot be ruled out, although the geochemical data suggest the waters are predominantly young. Fluid flow furthermore appears restricted to the shallow debris avalanche and pyroclastic deposits laid down during the May 18, 1980 eruption (Shevenell and Goff, 1995).

The relative importance of magmatic and meteoric waters to hydrothermal circulation is of interest for future monitoring efforts. Should circulation be fed primarily by surface recharge, it is difficult to differentiate rainfall-induced SP variations from those related to magmatic disturbances. To better constrain the role of meteoric recharge, repeat measurements taken along profile DD' during the 2001 field campaign are examined (Fig. 4).

No volcanic or unusual seismic activity was reported between the 2000 and 2001 surveys. Annual rainfall prior to the 2000 measurements was 100–125 cm and several snowfields were present on the north flank of the dome at the time of the survey. By comparison, precipitation in the year prior to the 2001 measurements amounted to only 60–70 cm, and the north face of the dome was free of snow during the survey. While repeat measurements were limited to one profile, little difference is observed in the SP field between successive years. There is some indication that the broad anomaly coincident with the dome is of larger spatial wavelength in 2001, possibly indicating growth (expansion) of the underlying hydrothermal system. It is unlikely, however, that this change is associated with meteoric recharge, as less precipitation occurred in 2001 than 2000.

Though infiltration of surface water into the volcano is expected to cause changes in self-potential, the time-

scale of such infiltration is unknown. The stability of the repeat measurements during years with variable rainfall and snowmelt suggests seepage occurs either on time scales of hours to days, in which case only a short-lived SP signature is expected, or on longer time scales of years to decades. Mastin (1994) examined the correlation between rainfall and explosive tephra emissions at Mount St. Helens and found significant correlation on time scales of 4–6 days, suggesting infiltration occurs rapidly. Modeling studies by Elsworth et al. (2004) of rainfall infiltration into the fractured andesitic dome of Montserrat (a close analog to the Mount St. Helens lava dome) further suggest times scales of hours are more appropriate. Since precipitation was absent in the two weeks prior to both surveys, no associated change in the SP field would be expected. It is thus likely that meteoric recharge acts as a short-term modulator of the stable background signal. During times of meteoric recharge, the negative anomaly on the lower flanks of the dome is likely enhanced, while the positive anomaly near the dome's summit is subdued.

Can the observed self-potential field be maintained by vapors exsolved from a cooling magma? By modeling the 1980–86 lava dome as a system open to continuous magmatic degassing, Shevenell and Goff (2000) estimate that as of 2000, roughly 63% of the water in the original 1980 magma remained in the melt. Thus a steady extraction of water vapor (which comprises ~95% of the magmatic volatiles; Rutherford and Devine, 1988) could potentially sustain hydrothermal circulation within the dome, as well as supply fumaroles and contribute to thermal springs within the breach. We propose a model in which hydrothermal circulation is generated and maintained by exsolved magmatic vapors, and modulated on short time scales (hours to days) by surface recharge (Fig. 5). Electrokinetic, rapid fluid disruption, and thermoelectric effects contribute to the observed positive anomaly near the dome summit, while downward flow within the flanks of the dome

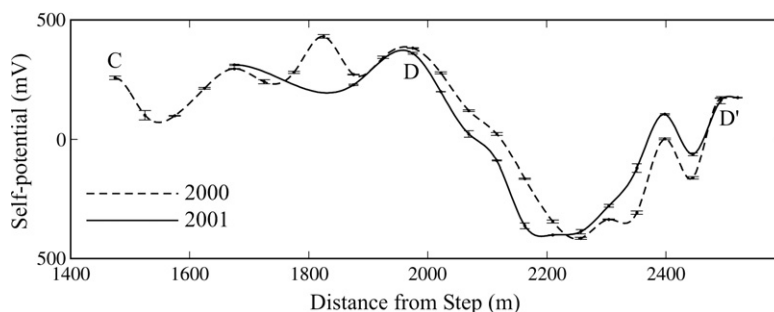


Fig. 4. Comparison of self-potential measurements made in 2000 and 2001 along profile CDD'. Note the close agreement at both short and long wavelengths despite significant differences in rainfall in 2000 and 2001.

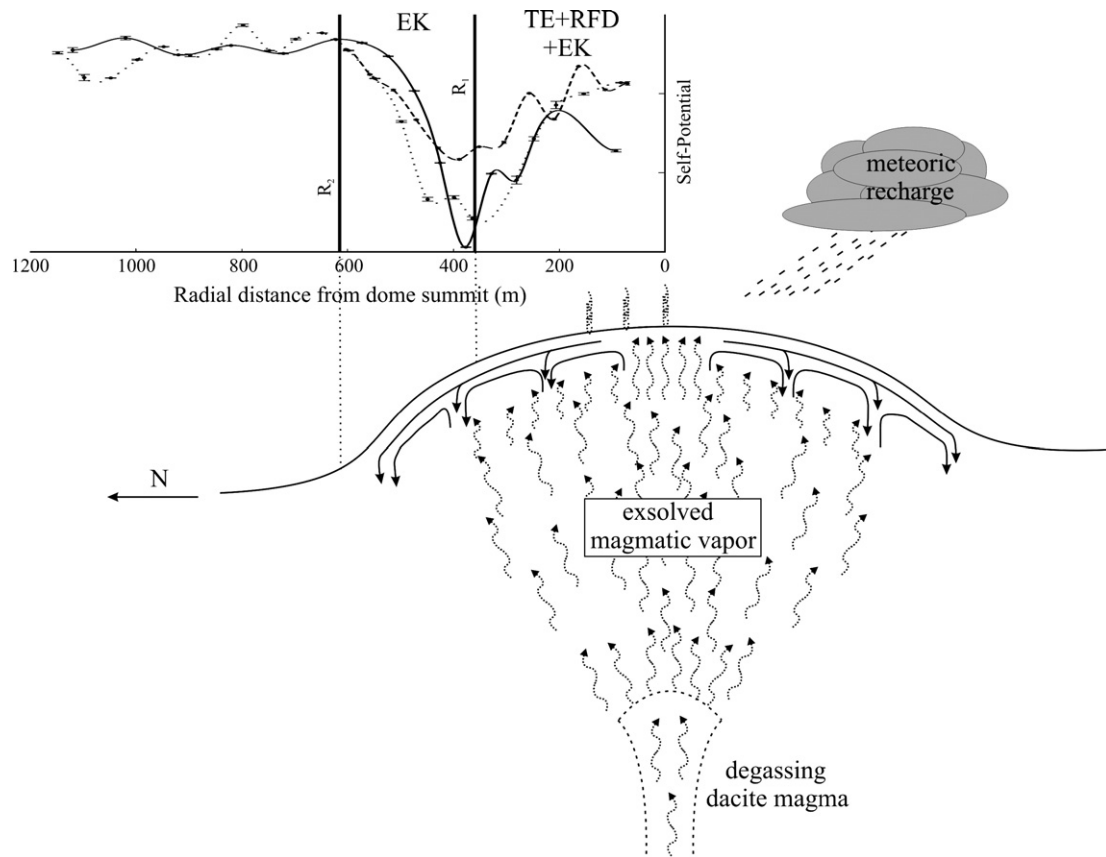


Fig. 5. Inferred hydrothermal circulation within the 1980–86 lava dome looking east. The hydrothermal cell gives rise to the measured dipolar self-potential anomaly, with rising potentials near the summit ($r < R_1$) and negative values on the lower flanks ($R_1 < r < R_2$). The extent of circulation may be on a dome-scale, as shown, or localized to the northern flank of the dome. Water vapor (dashed arrows) exsolved from a deep cooling magma condenses at shallow levels within the lava dome with return flow within and along the flanks of the dome (solid arrows). Circulation is likely modulated on short time-scales by meteoric recharge, giving rise to the mixed magmatic/meteoric signature of both dome fumarole condensates and thermal waters. There is limited system loss to Loowit and Step Creeks as well as dome fumaroles.

probably gives rise to the negative anomaly on the north flank. The composite nature of the dome, formed through a series of extruded lobes, may furthermore act to focus downward circulation along the boundaries of such extrusions. A zone of two-phase flow probably exists at the base of the fluid cell, where RFD is expected to contribute.

Though the degassing magma may reside deep within the conduit that supplied the 1980–86 dome, fluid convection is quite shallow (< 1.5 km), limited by the shallow vaporization isotherm. With our limited survey coverage, it is impossible to tell whether circulation is on a dome-scale, as depicted, or within one or more focused zones along the northern flank. Furthermore, it is difficult to quantify how much water is required to produce the measured SP signal. In the EK effect, the voltage generated scales with the applied pressure gradient, which via Darcy's Law is proportional to the volumetric flow rate. For a fixed flow rate it is the zeta potential, that determines

the magnitude and size of the resulting voltage. Studies of zeolitized volcanic materials found zeta potentials 2–3 times larger than in corresponding unaltered materials (Revil et al., 2002). This alteration, the result of chemical weathering of minerals by hot hydrothermal fluids, is observed at the surface, and is almost certainly occurring within the dome. This alteration, together with the high temperature of the dome, will tend to amplify the EK signature. Thus it is plausible that high volumetric flow rates are not required to generate the self-potentials observed.

The repeatability of SP measurements under varying surface conditions and their long-term stability with respect to rainfall are important for monitoring future activity at Mount St. Helens. The 2004–05 lava dome offers an opportunity to follow the establishment and development of a hydrothermal cell within a newly extruded dome. It further offers the possibility of

differentiating between the various generating mechanisms, as the EK effect is unlikely to contribute within the presumably dry, freshly extruded dome.

5. Conclusions

A dipolar self-potential anomaly was detected within the crater of Mount St. Helens. Data coverage was limited to the north flank of the 1980–86 dome, where the anomaly reaches peak values of -1 V on the lower flanks before reversing sign higher up. While this anomaly may be related to a previous vent location, its radial symmetry suggests it is part of a larger ring-shaped anomaly centered about the dome.

There is no evidence of a topographic effect. This may indicate a deep water table with weak topographically-driven flow or, alternatively, a shallow aquifer perched atop an impermeable flow boundary. A localized correlation between self-potential and topography observed on the lower flanks of the dome is probably of hydrothermal origin.

The dipole anomaly is attributed to the upward circulation of geothermal waters toward the apex of the dome with return circulation occurring further down the slopes, possibly channeled along boundaries between past extrusions. The measured anomaly is supportive of a dome-scale ring anomaly, though due to our limited coverage, we cannot rule out a more localized anomaly. The spatial wavelengths of an inferred ring anomaly (~ 1300 m diameter for the negative ring, and ~ 800 m for the positive disc) provide a maximum estimate of source depth, and indicate that hydrothermal circulation is shallow (<1.5 km). Fluid circulation within the dome of Mount St. Helens is very likely generated and maintained by waters from a degassing magma at depth, modulated on short time scales by meteoric influx. The long-term insensitivity of the SP field to precipitation changes suggests the self-potential method is an effective monitoring tool at Mount St. Helens.

Acknowledgements

This work is made possible by grants from the Geological Society of America, the USGS Cascade Volcano Observatory, the University of Washington Department of Earth and Space Sciences and the Natural Sciences and Engineering Research Council (NSERC) of Canada. This work has benefited greatly from discussions with Dan Dzurisin, Chris Newhall, and Steve Malone in addition to reviews by Shaul Hurwitz, Larry Mastin, and two anonymous reviewers. Thanks to the assistance of Peter Frenzen, Bruce Babb, and the staff of the Mount

St. Helens National Volcanic Monument. Special thanks to Jerry Casson, Jason Cooke, Chris Fuller, Taber Hersum, Betsy Meek, Pieter Mumm, and Arnd Junghans for all the hard work and good humor. Additional thanks to Stu Taft and Hillsboro helicopters.

References

- Aizawa, K., 2004. A large self-potential anomaly and its changes on the quiet Mt. Fuji, Japan. *Geophys. Res. Lett.* 31. doi:10.1029/2004GL019462.
- Aizawa, K., Yoshimura, R., Oshiman, N., Yamazaki, K., Uto, T., Ogawa, Y., Tank, S.B., Kanda, W., Sakanaka, S., Furukawa, Y., Hashimoto, T., Uyeshima, M., Ogawa, T., Shiozaki, I., Hurst, T., 2005. Hydrothermal system beneath Mt. Fuji volcano inferred from magnetotellurics and electric self-potential. *Earth Planet. Sci. Lett.* 235, 343–355.
- Aubert, M., Dana, I.N., Gourgaud, A., 2000. Internal structure of the Merapi summit from self-potential measurements. *J. Volcanol. Geotherm. Res.* 100, 337–343.
- Byrdina, S., Friedel, S., Wassermann, J., Zlotnicki, J., 2003. Self-potential variations associated with ultra-long-period seismic signals at Merapi volcano. *Geophys. Res. Lett.* 30. doi:10.1029/2003GL018272.
- Corwin, R.F., Hoover, D.B., 1979. The self-potential method in geothermal exploration. *Geophysics* 44, 226–245.
- Davis, P.M., Dvorak, J., Johnston, M.L., Dzurisin, D., 1989. Electric and magnetic field measurements on Mount St. Helens volcano at times of eruptions 1980–1985. *J. Geomagn. Geoelectr.* 41, 783–796.
- Dzurisin, D., Denlinger, R.P., Rosenbaum, J.G., 1990. Cooling rate and thermal structure determined from progressive magnetization of the dacite dome at Mount St. Helens, Washington. *J. Geophys. Res.* 95, 2763–2780.
- Elsworth, D., Voight, B., Thompson, G., Young, S.R., 2004. Thermal-hydrologic mechanism for rainfall-triggered collapse of lava domes. *Geology* 32, 969–972. doi:10.1130/G20730.1.
- Finizola, A., Sortino, S., Lénat, J.-F., Valenza, M., 2002. Fluid circulation at Stromboli volcano (Aeolian Islands, Italy) from self-potential and CO₂ surveys. *J. Volcanol. Geotherm. Res.* 116, 1–18.
- Finizola, A., Lénat, J.-F., Macedo, O., Ramos, D., Thouret, J.-C., Sortino, F., 2004. Fluid circulation and structural discontinuities inside Misti volcano (Peru) inferred from self-potential measurements. *J. Volcanol. Geotherm. Res.* 135, 343–360.
- Hase, H., Ishido, T., Takakura, S., Hashimoto, T., Sato, K., Tanaka, Y., 2003. ζ potential measurement of volcanic rocks from Aso caldera. *Geophys. Res. Lett.* 30. doi:10.1029/2003GL018694.
- Hashimoto, T., Tanaka, Y., 1995. A large self-potential anomaly on Unzen volcano, Shimbara peninsula, Kyushu island, Japan. *Geophys. Res. Lett.* 22, 191–194.
- Hurwitz, S., Kipp, K.L., Ingebritsen, S.E., Reid, M.E., 2003. Groundwater flow, heat transport, and water table position within volcanic edifices: implications for volcanic processes in the Cascade Range. *J. Geophys. Res.* 108. doi:10.1029/2003JB002565.
- Ishido, T., 2004. Electrokinetic mechanism for the “W”-shaped self-potential profile on volcanoes. *Geophys. Res. Lett.* 31. doi:10.1029/2004GL020409.
- Jackson, D.B., Kauahikaua, J., 1987. Regional self-potential anomalies at Kilauea volcano. “Volcanism in Hawaii” chapter 40. USGS. Prof. Pap., vol. 1350, pp. 947–959.

- Johnston, M.J.S., Byerlee, J.D., Lockner, D., 2001. Rapid fluid disruption: a source for self-potential anomalies on volcanoes. *J. Geophys. Res.* 106, 4327–4335.
- Johnston, M.J.S., Lockner, D., Byerlee, J.D., 2002. reply to comment by Revil on “Rapid fluid disruption: a source for self-potential anomalies on volcanoes” by M.J.S. Johnston, J.D. Byerlee, and D. Lockner. *J. Geophys. Res.* 107. doi:10.1029/2002JB001794.
- Lénat, J.-F., 1995. Geoelectric methods in volcano monitoring. In: McGuire, B., Kilburn, C.R.J., Murray, J. (Eds.), *Monitoring Active Volcanoes: Strategies, Procedures and Techniques*. University College London.
- Lipman, P.W., Mullineaux, D.R. (Eds.), 1981. *The 1980 Eruptions of Mount St. Helens*, Washington. USGS. Prof. Pap, vol. 1250.
- Major, J.J., Scott, W.E., Drieger, C., Dzurisin, D., 2005. Mount St. Helens Erupts Again, Activity from September 2004 through March 2005, United States Geological Survey Fact Sheet 2005–3036. 4 pp.
- Mastin, L.G., 1994. Explosive tephra emissions at Mount St. Helens, 1989–1991: the violent escape of magmatic gas following storms. *Geol. Soc. Amer. Bull.* 106, 175–185.
- Michel, S., Zlotnicki, J., 1998. Self-potential and magnetic surveying of La Fournaise volcano (Réunion Island): correlations with faulting, fluid circulation, and eruption. *J. Geophys. Res.* 103, 17845–17857.
- Nourbehecht, B., 1963. Irreversible thermodynamic effects in inhomogeneous media and their applications in certain geologic problems. Ph.D. Thesis, Mass. Inst. Technol., Cambridge.
- Nyquist, J., Corry, C., 2002. Self-potential: the ugly duckling of environmental geophysics. *Lead. Edge* 446–451.
- Pretorius, V., Hopkins, B.J., Schieke, J.D., 1974. Electro-osmosis: new concept for high-speed liquid-chromatography. *J. Chromatogr.* 99, 23–30.
- Revil, A., 2002. Comment on “Rapid fluid disruption: a source for self-potential anomalies on volcanoes” by M.J.S. Johnston, J.D. Byerlee, and D. Lockner. *J. Geophys. Res.* 107. doi:10.1029/2001JB000788.
- Revil, A., Schwaeger, H., Cathles III, L.M., Manhardt, P.D., 1999. Streaming potential in porous media 2. Theory and application to geothermal systems. *J. Geophys. Res.* 104, 20033–20048.
- Revil, A., Hermitte, D., Spangenberg, E., Cochemé, J.J., 2002. Electrical properties of zeolitized volcanoclastic materials. *J. Geophys. Res.* 107. doi:10.1029/2001JB000599.
- Revil, A., Finizola, A., Sortino, F., Ripepe, M., 2004. Geophysical investigations at Stromboli volcano, Italy: implications for ground water flow and paroxysmal activity. *Geophys. J. Int.* 157, 426–440.
- Rutherford, M.J., Devine, J.D., 1988. The May 18, 1980 eruption of Mount St. Helens 3. Stability and chemistry of amphibole in the magma chamber. *J. Geophys. Res.* 93, 11949–11959.
- Rutherford, M.J., Sigurdsson, H., Carey, S., Davis, A., 1985. The May 18, 1980, eruption of Mount St. Helens 1. Melt composition and experimental phase equilibria. *J. Geophys. Res.* 90, 2929–2947.
- Sasai, Y., Uyeshima, M., Zlotnicki, J., Utada, H., Kagiya, T., Hashimoto, T., Takahashi, Y., 2002. Magnetic and electric field observations during the 2000 activity of Miyaki-jima volcano, Central Japan. *Earth Planet. Sci. Lett.* 203, 769–777.
- Shevenell, L., Goff, F., 1993. Addition of magmatic volatiles into the hot spring waters of Loowit Canyon, Mount St. Helens, Washington, USA. *Bull. Volcanol.* 55, 489–503.
- Shevenell, L., Goff, F., 1995. Evolution of hydrothermal waters at Mount St. Helens, Washington, USA. *J. Volcanol. Geotherm. Res.* 69, 73–94.
- Shevenell, L., Goff, F., 2000. Temporal geochemical variations in volatile emissions from Mount St. Helens, USA, 1980–1994. *J. Volcanol. Geotherm. Res.* 99, 123–138.
- Swanson, D.A., Holcomb, R.T., 1990. Regularities in growth of the Mount St. Helens dacite dome, 1980–1986. In: Fink, J.H. (Ed.), *Lava Flows and Domes: Emplacement Mechanisms and Hazard Implications*. Springer.
- Swanson, D.A., Dzurisin, D., Holcomb, R.T., Iwatsubo, E.Y., Chadwick Jr., W.W., Casadevall, T.J., Ewert, J.W., Heliker, C., 1987. Growth of the lava dome at Mount St. Helens, Washington (USA). In: Fink, J.H. (Ed.), *The Emplacement of Silicic Domes and Lava Flows*. Special Paper, vol. 212. Geological Society of America.
- Thouret, J.-C., Finizola, A., Forani, M., Legeley-Padovani, A., Suni, J., Frechen, M., 2001. Geology of El Misti volcano near the city of Arequipa, Peru. *GSA. Bull.* 113, 1593–1610.
- Zlotnicki, J., Boudon, G., Viodé, J.P., Delarue, J.F., Mille, A., Bruère, F., 1998. Hydrothermal circulation beneath Mount Pelée inferred by self-potential surveying. Structural and tectonic implications. *J. Volcanol. Geotherm. Res.* 84, 73–91.